

Mitochondria-targeting nano therapy altering IDH2 mediated EZH2/EZH1 interaction as precise epigenetic regulation of Glioblastoma

Babita Kaundal, Surajit Karmakar ^{*a} and Subhasree Roy Choudhury^{*a}

Institute of Nano Science and Technology, Sector -81 Mohali, Punjab - 140306, India.

Supporting information

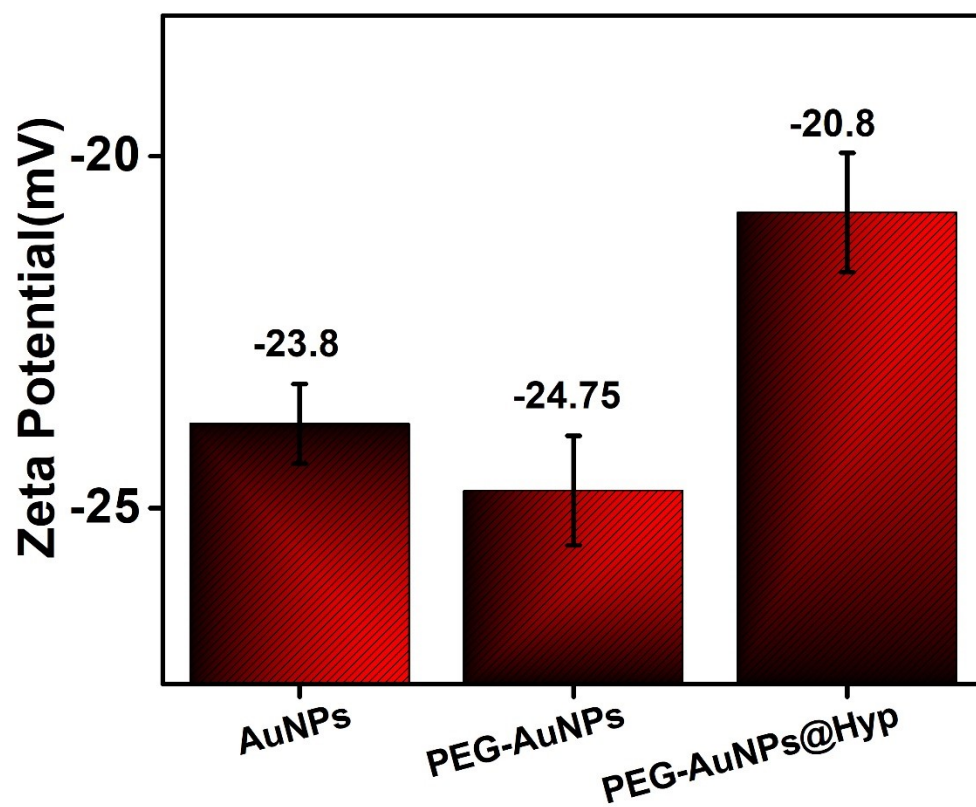


Fig. S1. After synthesis, the Zeta-potential values of the AuNPs, PEG-AuNPs, and PEG-AuNPs@hyp(B) were analyzed.

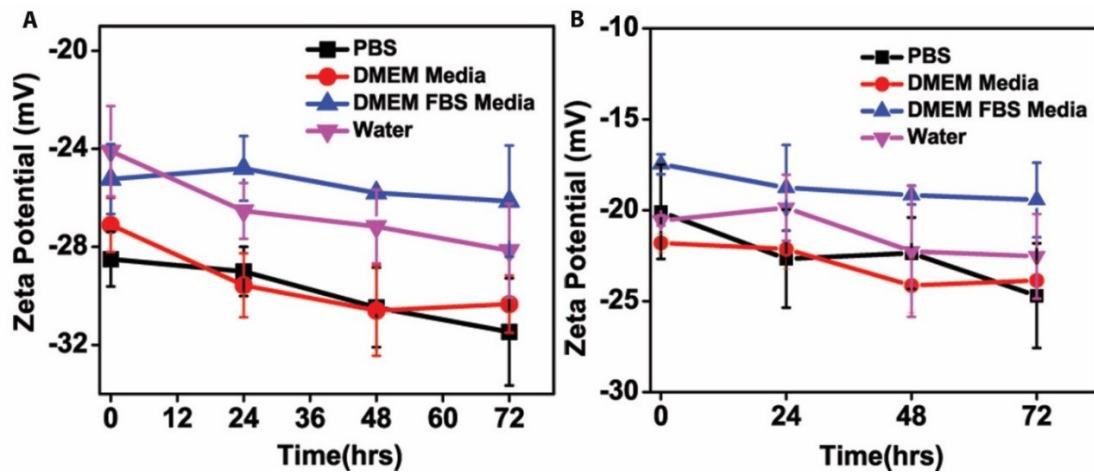


Fig. S2. The Zeta-potential values of the PEG-AuNPs (A) and PEG-AuNPs@hyp (B) in PBS, DMEM, DMEM + 10% FBS, and water, respectively, at different time points, show the stability of nanoformulation. The Student t-test at $*P < 0.05$ and one-way ANOVA with the Tukey test at the $**P < 0.01$ ($n = 3$) significance level is performed for statistical comparison.

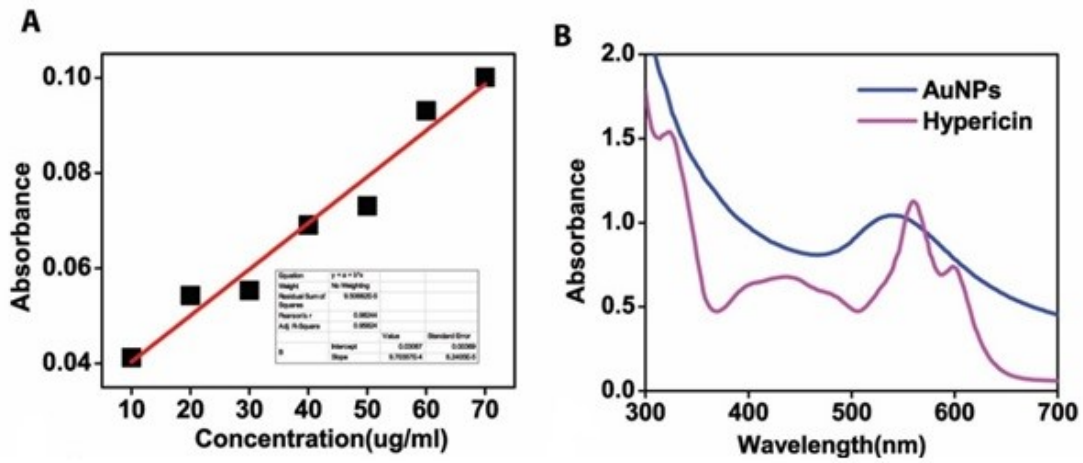


Fig. S3. The standard curve of the hypericin prepared with increasing the concentrations of hypericin prepared at absorbance @590 nm prepared (A); The absorbance of prepared PEG-AuNPs and hypericin by the UV Visible spectroscopy (B).

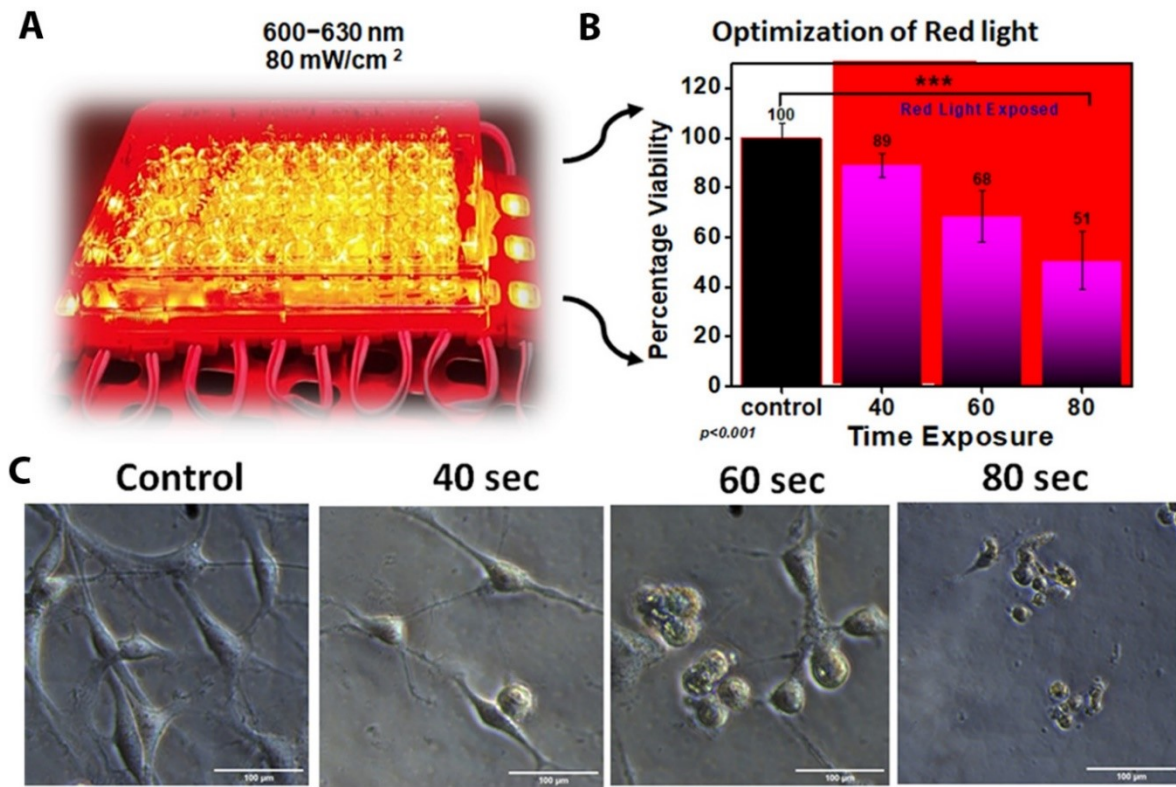


Fig. S4 The Exposure of red light at different time intervals with 80 mV power to the glioblastoma cell line(A); IC50 of light exposure optimization(B); and morphology characterization after 24 hrs of light exposure using an optical microscope (C).

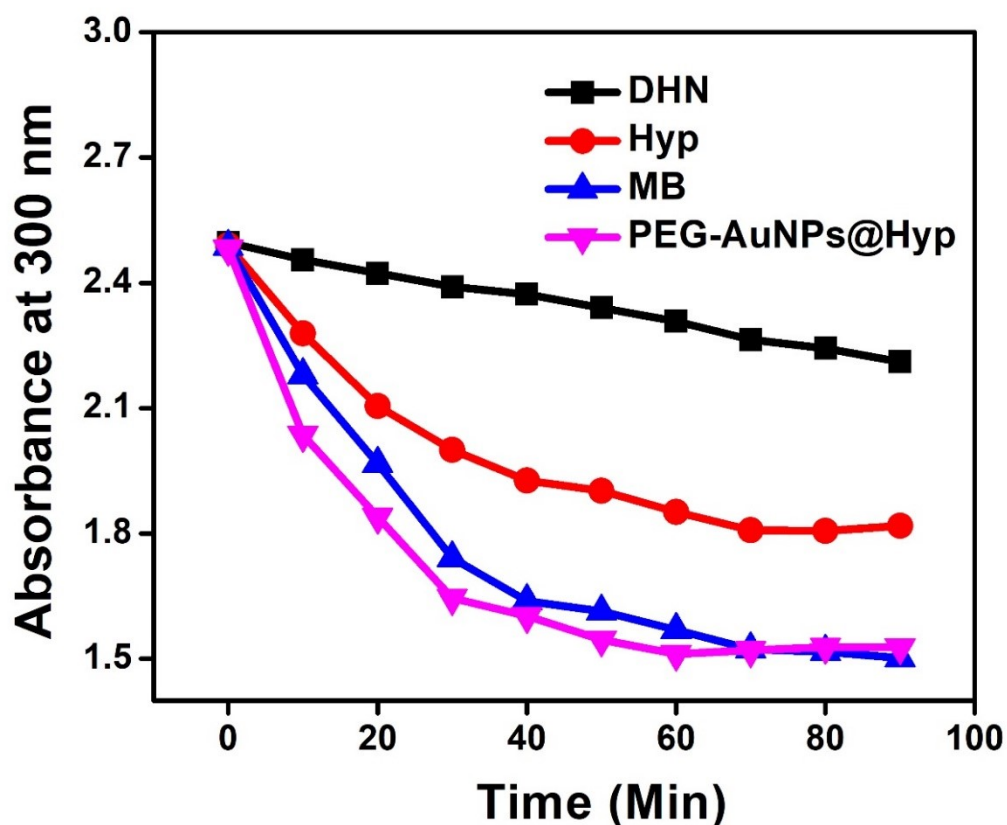


Fig. S5. The singlet oxygen production efficiency of the PEG-AuNPs@Hyp, 1,5-dihydroxy naphthalene (DHN), Methylene blue (MB), and Hypericin(Hyp) at 300 nm in the presence of irradiation time under ambient conditions.

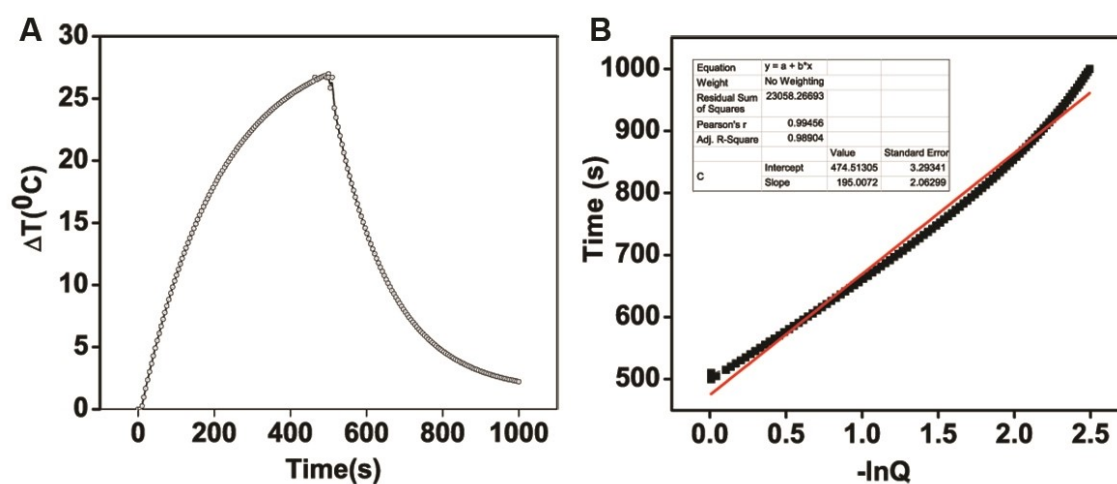


Fig. S6. Heating and cooling curve of PEG-AuNPs@Hyp with or without irradiation (600-630 nm, 80 mW/cm²)(A); Linear fitting of $-\ln\theta$ and time(B).

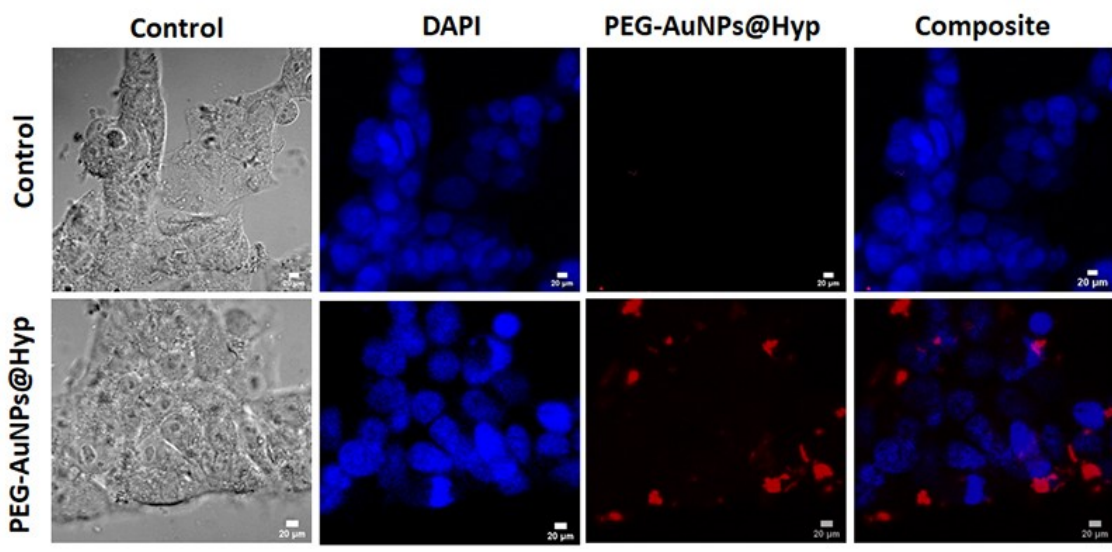


Fig. S7. The Cellular uptake of the nanoformulation in HEK293T cell after exposure to red light at different time intervals with 80 mV power to the glioblastoma cell line.

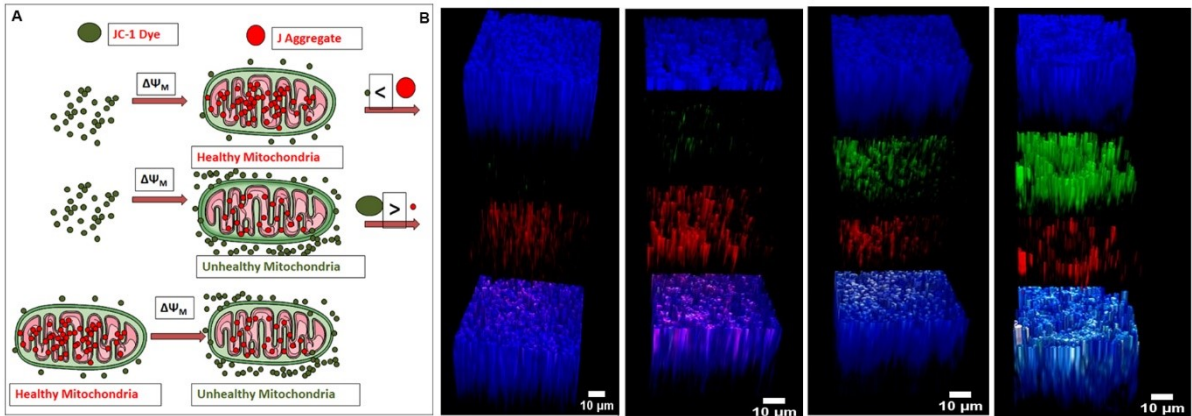


Fig. S8. The schematic shows the JC-1 mechanism in analyzing mitochondria membrane potential (A). The mitochondria membrane potential analysis in the 3D raft model of the LN18 GBM cells was analyzed by JC-1 dye with treatment to different groups (B).

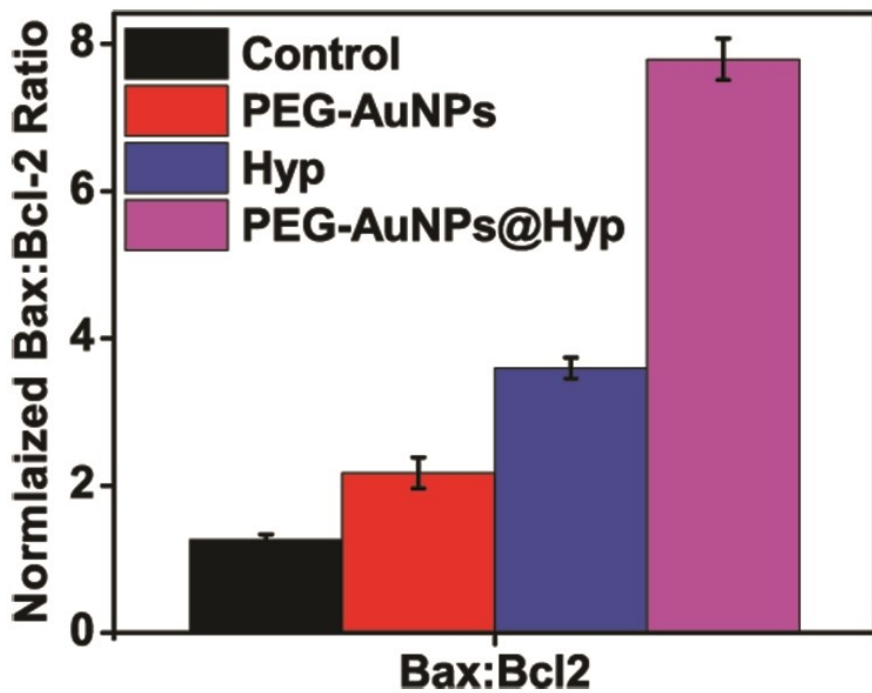


Fig. S9. The Bax: Bcl2 ratio showing from the western blot analysis.

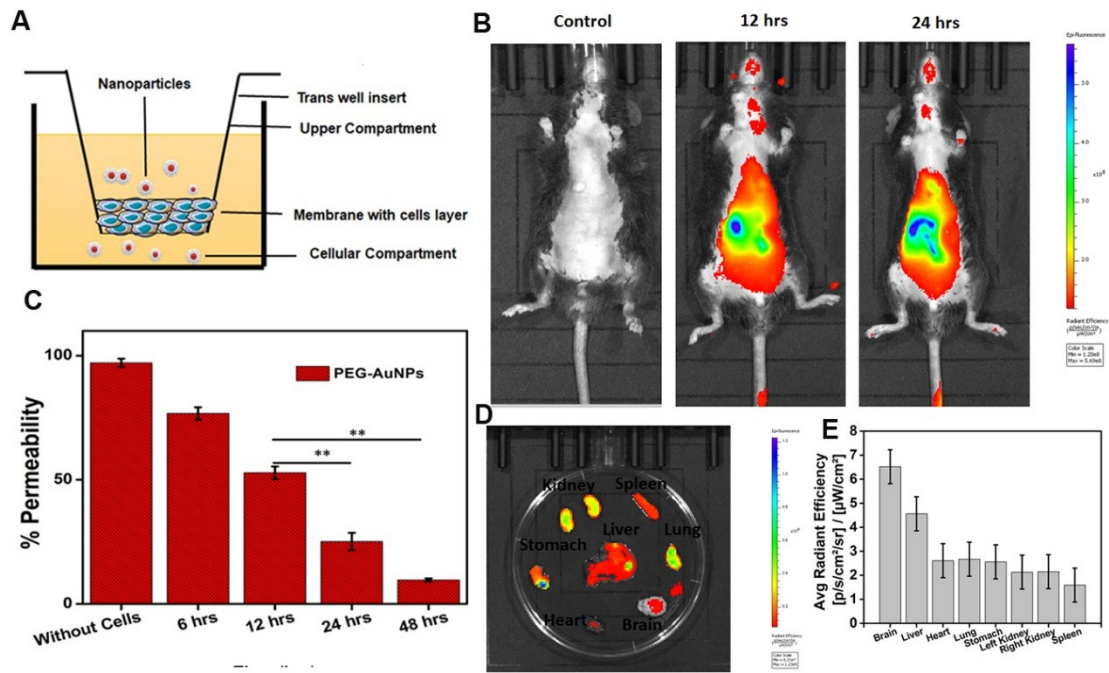


Fig. S10. Biodistribution of PEG-AuNPs@Hyp nanoparticles used for whole animal imaging 12 and 24 hrs post intravenous injection (A); ex vivo imaging of organs harvested after injection (C); the organs (from top left to bottom right) are brains, heart, liver, lung, stomach, right kidney, left kidney, and spleen; the quantification of relative fluorescence (D).

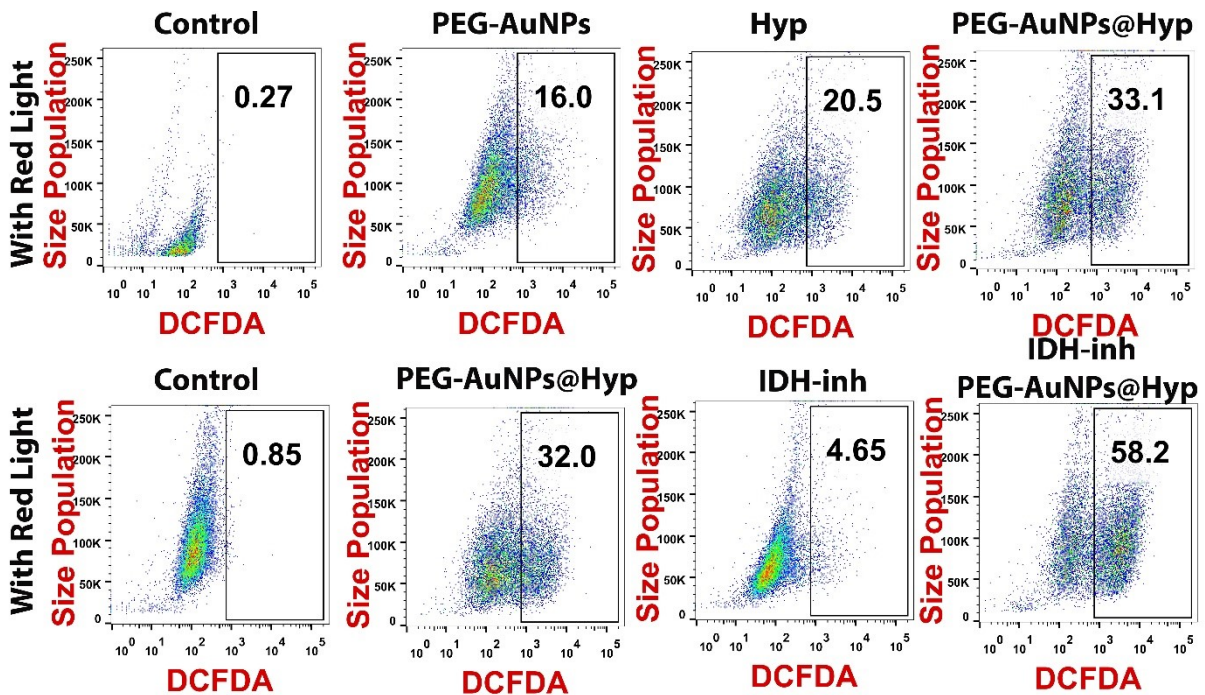


Fig. S11. The ROS generation from the in vivo tumor single-cell suspension analyzed by flow cytometry

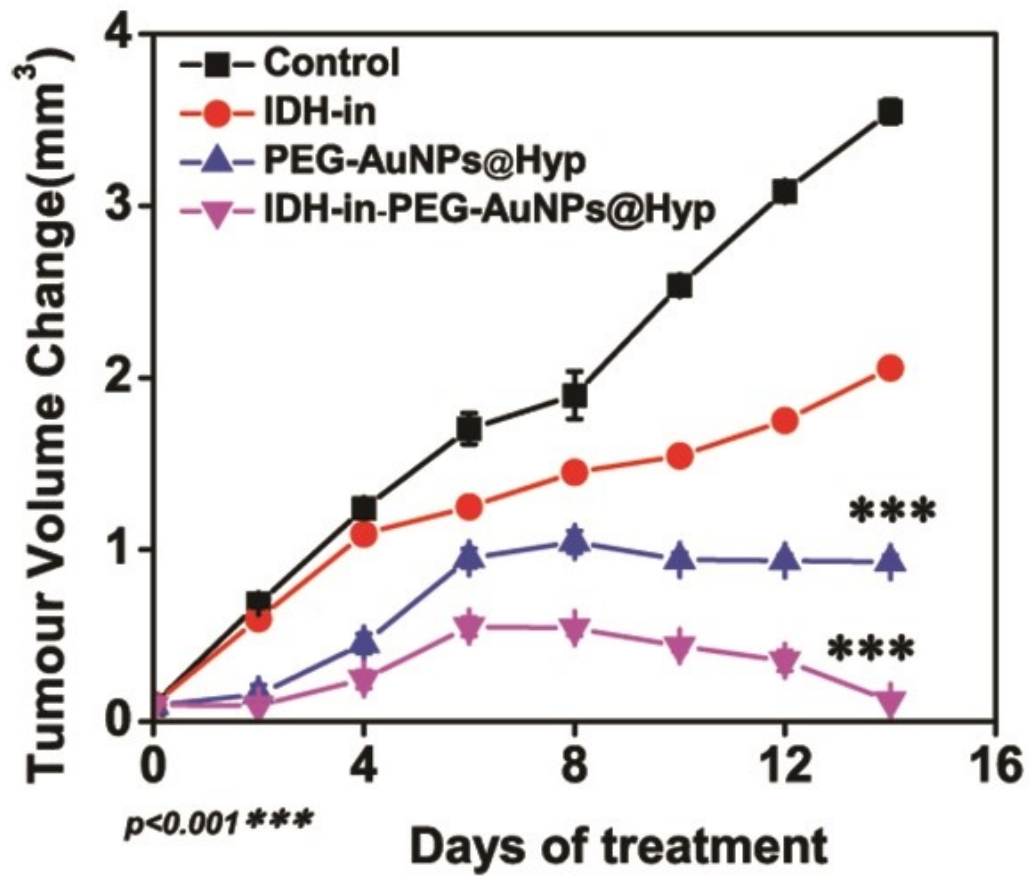


Fig. S12. The Develop GBM Tumor volume change during the treatment process